



RDF pyrolysis by TG-FTIR and Py-GC/MS and combustion in a double furnaces reactor

Xiaolin Chen^{1,2} · Junlin Xie^{1,3} · Shuxia Mei^{1,2} · Feng He^{1,2} · Hu Yang^{1,2}

Received: 7 February 2018 / Accepted: 18 August 2018 / Published online: 28 August 2018
© Akadémiai Kiadó, Budapest, Hungary 2018

Abstract

With the increasing depletion of fossil energy, the refuse-derived fuel (RDF) as an unavoidable by-product of human activities has been used as an alternative fuel in the precalciner cement kilns. Since the RDF combustion also brings the problems of NO_x pollution, it is quite important to find ways to lower the NO_x emission during RDF combustion in the precalciner. The pyrolysis characteristics and products of RDF were studied by TG-FTIR and Py-GC/MS. From TG-FTIR and Py-GC/MS tests, various carboxylic acids and alkenes formed with NO_x released at the RDF pyrolysis process at 200–550 °C. By simulating the temperature (700 °C, 800 °C and 900 °C) and O₂ (12%, 14%, 16%, 18% and 21%) environment of the precalciner using a double furnaces reactor, the combustion processes and NO_x formation characteristics of RDF combustion were studied. The results showed that the volatile-N was the dominant reactant source of fuel NO_x during RDF combustion. The fuel-N conversion and NO_x emission yield showed a continuous decreasing trend with temperature increasing from 700 to 900 °C. The fuel-N conversion and NO_x emission yield showed a slight increasing trend with the oxygen concentration increase, and the optimum oxygen concentration for RDF combustion was 14%. In this study, the optimum temperature was 900 °C and oxygen concentration was 14% for de-NO_x in the precalciner.

Keywords TG-FTIR · Py-GC/MS · RDF · Pyrolysis · Combustion · NO_x

Introduction

With the increasing depletion of limited fossil fuel and the continuous generation of municipal solid waste, RDF, which is an alternative fuel from municipal solid waste, is gaining more and more attention in cement industry [1–3]. As a key thermal equipment in cement industry, the precalciner is the major facility for dealing with RDF. It will result in NO_x emission during RDF combustion just like the coal combustion. With the more and more serious air

pollution, emission regulations have become increasingly stringent. Therefore, to realize the optimized utilization of RDF, it is quite urgent to study the mechanism of low NO_x emission and the associated factors during RDF combustion in the precalciner.

Thermogravimetric analysis (TG) has been widely used to characterize the thermal and kinetic processes of the combustion and pyrolysis of coal, RDF and other materials. Garcia and Lin have indicated that the pyrolysis model for RDF is composed of two independent models: one is the pyrolysis of fiber, and the other is the pyrolysis of plastic [4, 5]. Yi found that synergy exists between the biomass and biochar, and better combustibility is feasible by co-firing biochar with biomass [6]. Most of them focused on the kinetic parameters for characterization of fuels by TG, but ignored the specific gaseous product during of fuel pyrolysis and combustion [7, 8]. By using TG-FTIR and Py-GC/MS, the gaseous products could be gained during pyrolysis and combustion [9]. Thus, the pyrolysis characteristics of RDF were intended to be evaluated by using TG-FTIR and PY-GC/MS (6890 N) analysis in this paper.

✉ Shuxia Mei
msx0303@163.com

¹ State Key Laboratory of Silicate Materials for Architectures, Wuhan University of Technology, Wuhan 430070, People's Republic of China

² School of Materials Science and Engineering, Wuhan University of Technology, Wuhan 430070, People's Republic of China

³ Research and Test Center of Materials, Wuhan University of Technology, Wuhan 430070, People's Republic of China

The temperature environment and gas atmosphere in the thermal equipment have great influences on the combustion characteristics and NO_x formation process during RDF combustion. Some scholars have studied the RDF combustion characteristics. Stanislav Honus investigated the pyrolysis gaseous components of brown coal, biomass and rubber, respectively, from 500 to 650 °C, and found that there was no distinctive linear relationship between the average abundance of CO and NO_x [10]. Zhou studied the NO_x formation factors during biomass combustion from 900 to 1200 °C and found that a high combustion temperature may significantly reduce the char-NO reaction [11]. Qian studied the biomass combustion under oxygen-rich and found NO_x concentration increased from 80 to 140 ppm with temperature increasing from 700 to 900 °C, NO_x emission decreased with excess air ratio [12]. Duan found the NO_x emission of sawdust combustion increased from 7 to 69 ppm when the excess oxygen ratio increased from 40 to 70% [13]. Francisco performed the RDF combustion in a fluidized bed combustor, a slight decrease in the NO_x concentration was observed upon injection of secondary air [14]. In general, the experiments on different RDF combustion showed that the NO_x emission concentration was connected with temperature and O₂ concentration, but the NO_x emission concentration increase rates were different in different conditions [15–18].

As a complex high-temperature reactor, there occur gas–solid dispersion, pulverized coal combustion and calcium carbonate decomposition in the precalciner. The characteristics of the precalciner environment are special and mainly reflected in two aspects. Firstly, the precalciner is a large-scale reactor, which includes the endothermic reaction of coal combustion and the exothermic reaction of CaCO₃, resulting in the different temperatures distribution. And the average temperature in the precalciner is about 880 °C [19, 20]. Secondly, there are two types of gas flows in a precalciner, one is the tertiary air, in which the O₂ concentration is 21%; the other one is the flue gas from the rotary kiln, in which the O₂ concentration was from 2 to 4%, resulting in the different O₂ concentrations in different zone of the precalciner. And the average O₂ concentration in the main burning area is about 18%. Since the temperature and O₂ concentration are two main factors associated with NO_x emission during RDF combustion in precalciner, it is important to obtain a deep understanding of the combustion characteristics and NO_x formation process during RDF combustion in the high-temperature environment and complex gas atmosphere of the precalciner. What is more, to make clear the influences of temperature and O₂ concentration on NO_x emission is quite necessary.

Therefore, the combustion characteristics of one RDF taken from a cement plant were studied in a self-developed double furnaces reactor. To simulate the steady high-

temperature gas flow, we set two furnaces to ensure that the gas flow has been preheated effectively in the fixed-bed reactor experiments, which could prolong the residence time of the high-temperature gas flow and simulate the high-temperature environment in the precalciner better. And the mutual effect among CO, CO₂ and NO_x was analyzed during the whole combustion process. The results will provide theoretical reference for low NO_x combustion of RDF in the precalciner.

Experimental

Preparation of fuels

The RDF was gained from an actual cement industry and was the municipal solid waste from a city in China, which was milled and sieved to the size of < 180 μm before experiments. The proximate analysis conducted according to national standards (GB/T 212-2008). Carbon (C), oxygen (O), hydrogen (H), nitrogen (N) and sulfur (S) are the main chemical elements in a fuel. Thus, C, H, O, N and S content of the samples were determined by ultimate analysis conducted by Vario EL club analyzer. Calorific value of RDF was determined by the oxygen bomb calorimeter; each sample was tested at least three times and then took an average. All results were reported on air-dry basis. The proximate and ultimate analyses and calorific value of RDF are shown in Table 1.

Apparatus and methods

Pyrolysis experiments

Pyrolysis experiments were performed by using TG-FTIR (American Discovery TG and Nicolet 6700 Fourier transform infrared spectrometry) and PY-GC/MS (ENTECH 7100-CDS 5150-Agilent 6890N/5975) analysis. TG analysis, coupled with FTIR, is a good means by which to study not only the mass-loss characteristics and kinetics parameters of the thermal decomposition process, but also identify the volatile components generated in real time. Pyrolysis analysis was performed by using FTIR. Using a constant heating rate of 20 °C min⁻¹ in N₂ atmosphere, the samples were heated from 30 °C to 1000 °C. The HI-resolution sensitivity was 1.0 and HI-resolution ramp 20 °C min⁻¹ to 1000 °C. The spectral region of the FTIR was 4 cm⁻¹ and 4000–400 cm⁻¹, and the spectrum scan was conducted with 8 s intervals. The PY-GC/MS results could supplement the gas components. The carrier gas was helium, its flow rate was 1.0 mL min⁻¹, and the injection volume was 1 μL, the refractive ratio of distillation was 100:1. MS conditions were as follows: electron impact ion

Table 1 Proximate analysis and ultimate analysis of samples

| Sample | Proximate analysis/mass% | | | | Ultimate analysis/mass% | | | | | $Q_{\text{net, daf}}/\text{MJ kg}^{-1}$ |
|--------|--------------------------|-----------------|-----------------|--------------------|-------------------------|-----------------|-----------------|-----------------|-----------------|---|
| | M_{ad} | A_{ad} | V_{ad} | $F_{\text{c, ad}}$ | C_{ad} | H_{ad} | O_{ad} | N_{ad} | S_{ad} | |
| RDF | 3.6 | 48.75 | 46.9 | 0.75 | 36.78 | 4.36 | 4.57 | 1.16 | 0.78 | 12,421.80 |

source, transmission line temperature of 280 °C, ion source temperature of 230 °C, quadrupole temperature of 150 °C and mass scan range of 30–600 m/z.

Combustion experiments

The RDF combustion experimental system as shown in Fig. 1 included gas system, double-tube furnaces and flue gas analyzer. The tube furnace was OTF-1200X, which used a quartz tube as heating element; the adjustable temperature range was from room temperature to 1200 °C. The temperature was electrically controlled and displayed by a device automatically. N_2 and O_2 mixtures controlled by mass flow meters were used for combustion gas. The mixed gas was preheated in 1# furnace and then flowed into 2# furnace, which could maintain the stable high temperature during RDF combustion. In each experiment, the fuel sample was placed in a ceramic boat and rapidly pushed into the quartz tube which was already preheated to the desired temperature. For each run, the amount of fuel sample was about 500 mg and the gas flow rate was maintained at 1000 mL min^{-1} . The combustion flue gas, O_2 , CO_2 , CO and NO_x concentrations were monitored online by MGA5 flue gas analyzer continuously. The device measured the concentrations of O_2 and CO_2 with an infrared (IR) cell as volume percentages; concentrations of other gas were measured electrochemically in ppm. The time interval of sampling was 1 s. The yields of CO , CO_2 and NO_x can be calculated respectively by the integration of gas curves with time according to formula 1:

$$m_j = \sum_{i=1}^n c_i \times 10^{-6} \times v \div 60 \times t \times M_j \div 22.4 \quad (1)$$

In which m_j is the CO , CO_2 or NO_x yield (mg), C_i is the CO , CO_2 or NO_x concentration (ppm), v is the volumetric flow 1000 (mL min^{-1}), M_j is the molar mass of CO , CO_2 or NO_x , t is the time interval of sampling 1 (s), n is the number of being measured point, and j is CO , CO_2 or NO_x .

According to the NO_x yield, the fuel-N conversion can be calculated:

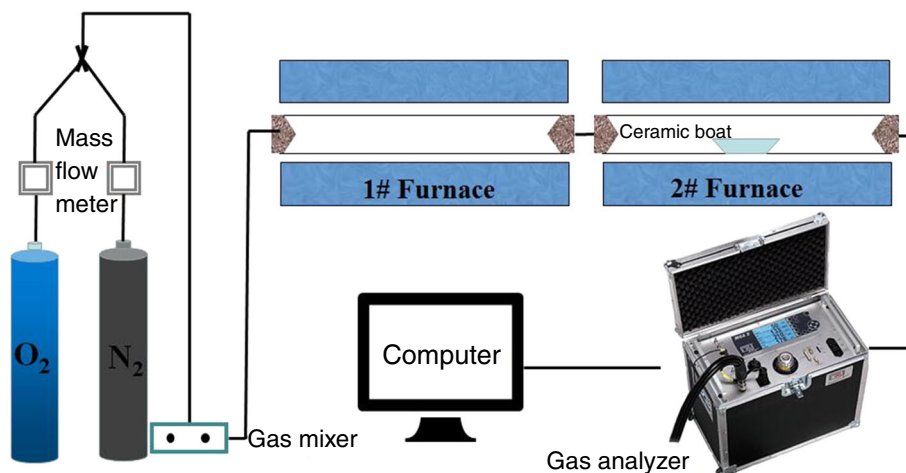
$$X_{\text{NO}_x} = \frac{m_{\text{NO}_x} \times \frac{14}{30}}{m_o \times N_{\text{ad}} \times (m_{\text{CO}_2} \times \frac{12}{44} + m_{\text{CO}} \times \frac{12}{28}) \div C_{\text{ad}} \div m_o} \quad (2)$$

In which X_{NO_x} is the fuel-N conversion (%), m_o is the mass of the fuel sample 500 (mg), N_{ad} is the N content in the fuel sample (mass%), and C_{ad} is the C content in the fuel sample (mass%).

Results and discussion

Properties of RDF pyrolysis

Pyrolysis is an important sub-step to study the combustion process. TG coupled with FTIR is a good means by which to study not only the mass-loss characteristics of the thermal decomposition process, but also identify the volatile components generated in real time. The pyrolysis characteristics, both the mass loss (TG curve, in unit of

Fig. 1 Double furnaces reactor

mass loss%) and the rate of mass loss (DTG curve, in unit of mg s^{-1} , derivative thermogravimetry) curves of RDF pyrolysis, are shown in Fig. 2. The corresponding FTIR spectrum is shown in Fig. 3. The PY-GC/MS test results of gas components during pyrolysis at different temperatures are listed in Table 2.

The RDF pyrolysis process could be divided into three stages according to Fig. 2. The first stage mass loss occurred early in the temperature of 30–200 °C. The mass percentage of pyrolysis residue was slight, which was about 2.2%. The typical volatile components in this stage are identified in Fig. 3a. The small molecular gaseous components (e.g., H_2O and CO_2) were easily identified by their prominent characteristic bands. The vibration peaks of C–H bonds and C=O bonds were detected at 1200–2000 cm^{-1} . According to the PY-GC/MS results, these were carboxylic acids ($\text{C}_{12}\text{H}_{24}\text{O}_2$, $\text{C}_{14}\text{H}_{28}\text{O}_2$, $\text{C}_{15}\text{H}_{30}\text{O}_2$, $\text{C}_{16}\text{H}_{32}\text{O}_2$, $\text{C}_{19}\text{H}_{36}\text{O}_2$). This stage was the drying process and the decomposition of some biomass components [21–23].

The second stage was the maximum mass loss focused at 200–550 °C. There were two distinct peaks at 378 °C and 499 °C in DTG curve as shown in Fig. 2. The small molecular gaseous components (e.g., H_2O , NO, CH_4 and CO_2) were easily identified at 378 °C. The nitrogen compounds were oxidized in this stage. CH_4 came primarily from the decomposition of carboxylic acids as listed above. The large amount of CO_2 was formed via the decarboxylation reaction and the breakage of carboxylic acids groups. Combining with Table 2 and Fig. 3, at 378 °C the hydrocarbons at 1200–2000 cm^{-1} were the stretching vibration peaks of carboxylic acids ($\text{C}_2\text{H}_4\text{O}_2$, $\text{C}_8\text{H}_{14}\text{O}_2$) and alkenes (C_8H_{16} , C_9H_{18}). At 499 °C, obvious CO peaks were detected, which showed the hydrocarbons could be further changed with temperature increasing. In the second stage, the mass loss was about 38.8%. The volatiles content was 46.9% as shown in Table 1. In this stage most of volatiles were released.

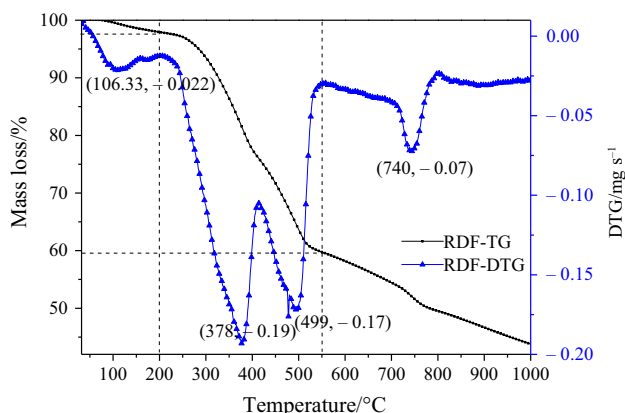


Fig. 2 TG and DTG curves of RDF pyrolysis

In the third stage (> 550 °C), there was an absorption peak at 740 °C. As shown in Fig. 3b and Table 2, the small molecular gaseous components (e.g., H_2O , CH_4 and CO_2) and macromolecular matters (e.g., benzene, methylbenzene and some other aromatic hydrocarbons) were easily identified. The IR characteristics peaks of CO_2 were quite obvious at 740 °C. That is because many stable macromolecular matters released in this stage and some carbonate decomposed. In this stage, the mass loss was about 15.12%.

In conclusion, a plenty of volatiles began to release at about 200 °C and the release of NOx mainly occurred in the second stage (200–550 °C) during RDF pyrolysis. In the present experimental conditions, the temperature was below 1500 °C, the formation of thermal NOx and prompt NOx was negligible, and all of the NOx emissions were considered to be from nitrogen compounds [24–28]. Then, at 700 °C, 800 °C and 900 °C, the fuel-N in RDF could release effectively. Meanwhile, a large amount of carboxylic acids and alkenes formed with NOx. The hydrocarbon could inhibit NOx production and promote the de-NOx. Thus, RDF is a meaningful alternative fuel for de-NOx in cement industry.

RDF combustion characteristics

Figure 4a is the gas release curve of RDF combustion at 900 °C. Figure 4b is the gas release rate curve, which is the derivative curve of Fig. 4a.

As shown in Fig. 4a, the RDF combustion product was mainly CO_2 ; the maximum concentration was 8.12%. The amount of CO and NOx was relatively low. According to Fig. 4a, the RDF combustion process could be hard to clearly distinguish between the homogeneous combustion of volatiles and the heterogeneous combustion of char. Based on the CO_2 release rate curve, as shown in Fig. 4b, RDF combustion process could be classified into two stages. The first stage ($t < 200$ s) was the volatiles release and combustion. In this stage, the CO, CO_2 and NOx were released and O_2 was consumed gradually, and their release peaks formed rapidly. Among of them, the CO released rapidly and formed release peak ($t = 62$ s). The CO release peak was the most sharpest, which showed the CO formation reaction was the fastest. The CO_2 began to release after CO release, and the CO_2 peak formed later ($t = 79$ s), the time of CO_2 release was longer than the CO formation time. The NOx release start point was the latest ($t = 100$ s), and the formation rate was the slowest, which showed the NOx formation reaction was the slowest and the CO could inhibit the NOx formation. So the equations are as follows:



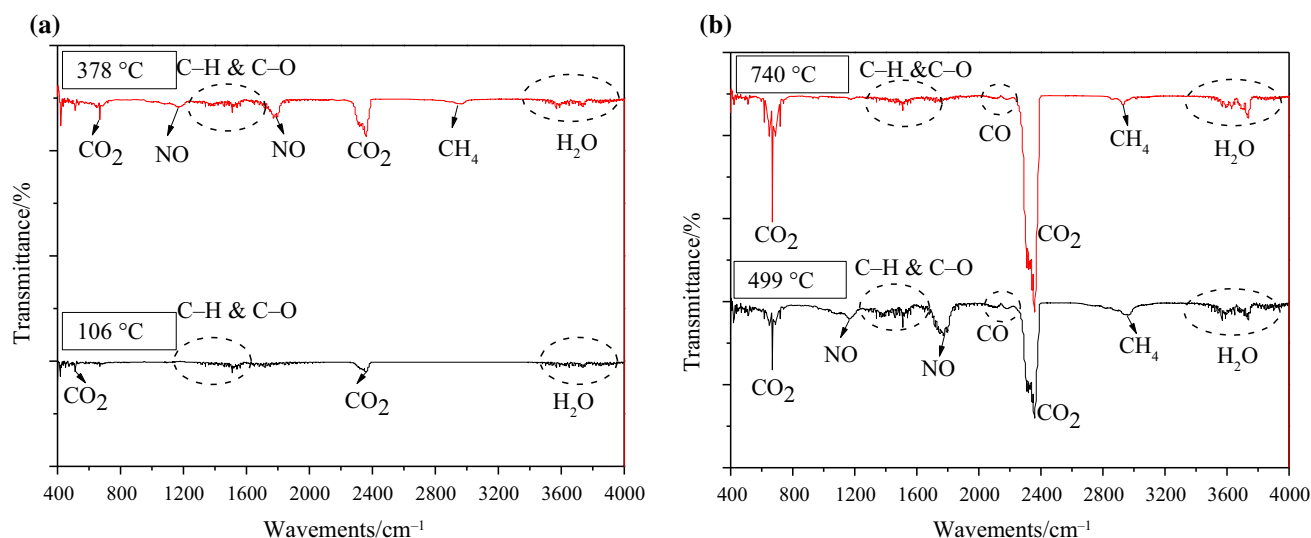


Fig. 3 FTIR spectrum of RDF pyrolysis at different temperature

Table 2 PY-GC/MS pyrolysis products of RDF

| Sample | ~200/°C | 200–550/°C | 550–900/°C |
|--------|--|--|--|
| RDF | CO ₂ , carboxylic acids (C ₁₂ H ₂₄ O ₂ , C ₁₄ H ₂₈ O ₂ , C ₁₅ H ₃₀ O ₂ , C ₁₆ H ₃₂ O ₂ , C ₁₉ H ₃₆ O ₂) | CO ₂ , carboxylic acids (C ₂ H ₄ O ₂ , C ₈ H ₁₄ O ₂), alkenes (C ₈ H ₁₆ , C ₉ H ₁₈) | alkenes (C _n H _{2n}), benzene (C ₆ H ₆), methylbenzene (C ₇ H ₈), styrene (C ₈ H ₈), naphthalene (C ₁₀ H ₈) |



The second stage ($t > 200$ s) was the char ignition combustion stage. In this stage, the CO₂ and CO concentration decreased continually and the reduction rate decreased. That is because part of char began to burn and some CO₂ and CO formed in this stage which could inhibit the concentration decreasing. In this part, NO_x kept forming, the NO_x release time lasted for about 350 s (200–550 s), but the release rate was quite slow. During the whole combustion process, the CO formed more easily than CO₂ and NO_x. That is because at high temperature, volatiles released rapidly resulting in a reductive atmosphere, which was beneficial to the CO release. The release curves of NO_x were similar to that of CO₂.

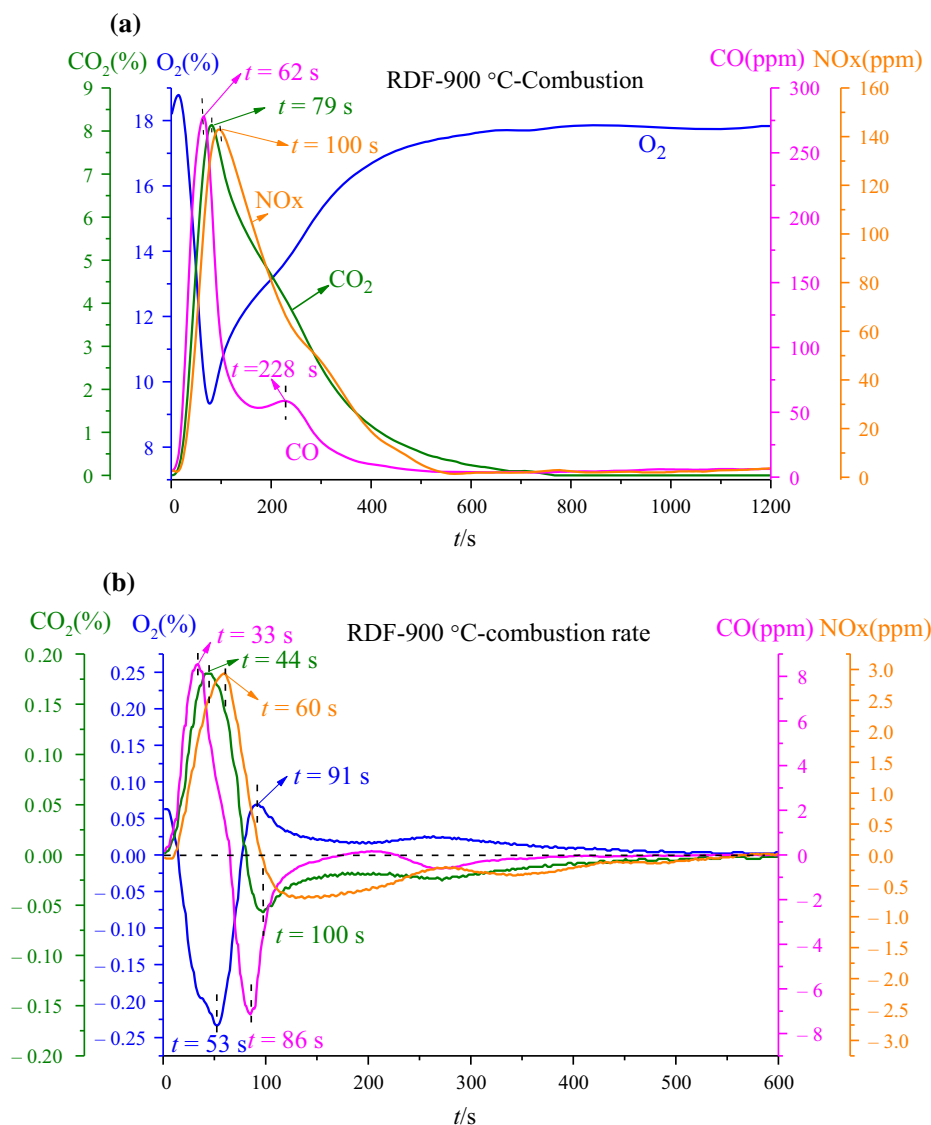
According to the above results, in the RDF combustion the volatiles release and combustion process was the primary stage, and the volatile-N was the dominant reactant source of NO_x emission. CO formed easily than volatile NO_x, and the NO_x concentration increased to the maximum with CO decrease.

Effects of temperature on NO_x emission

Figure 5 is the gas emission curves at different temperatures during RDF combustion. Figure 6 is the gas yields at different temperatures during RDF combustion. Figure 7 is the fuel-N conversion to NO_x during RDF combustion at different temperatures.

In general, the variation trends of CO release curves at different temperatures were similar, so were the CO₂, NO_x, O₂ curves. At 700 °C, the combustion rate was the slowest. The CO, CO₂ and NO_x peaks formed at $t = 129$ s, 98 s and 124 s, respectively. The whole combustion time was quite long, about 1164 s. The NO_x yield was the highest (as shown in Figs. 5c, 6). At 800 °C the reaction rate was quicker than at 700 °C. The CO, CO₂ and NO_x peaks formed at $t = 114$ s, 90 s and 112 s, respectively. The whole combustion time was about 913 s. At 900 °C, the reaction rate was the quickest. The CO, CO₂ and NO_x peaks formed at $t = 62$ s, 79 s and 100 s, respectively. The whole combustion time was about 768 s. The CO maximum decreased with temperature increasing, the CO₂ maximum increased with temperature increasing (as shown in Fig. 5a, b). The O₂ concentration curves showed that the higher the temperature, the quicker the combustion rate was (as shown in Fig. 5d). In conclusion, the combustion

Fig. 4 Gas release curve and gas release rate curve of RDF combustion at 900 °C. **a** Gas release curve, **b** gas release rate curve



efficiency was better at high temperature. The NO_x maximum was 202 ppm at 800 °C, which showed that there was no distinctive linear relationship between the NO_x maximum and temperature. Because at low temperature, a large amount of CO formed (maximum was 2168 ppm) and the combustion rate was quite slow, which could inhibit the volatile NO_x formation and NO_x formed could be reduced by CO; at high temperature, the CO yield was less, the combustion rate was rapid (as shown in Fig. 5d), and nitrogen compounds could not be oxidized into NO_x in time.

According to Figs. 6 and 7, the CO₂ yield was about 580 mg at different temperatures, which were two orders of magnitude higher than that of CO and NO_x yield. It showed that RDF burnt completely at different temperatures. The NO_x yield and fuel-N conversion ratio decreased with temperature increasing. At low temperature, the

combustion rate was slow and fuel-N could be oxidized into NO_x. The CO and NO_x reaction rate was slow at low temperatures; most of CO and NO_x went out with the gas flow and then be detected by the flue gas analyzer. What is more, RDF was a kind of fuel with high volatiles, and the combustion rate was quite rapid, only when at a low temperature the nitrogenous compounds could be oxidized effectively.

In general, there was distinctive linear relationship between the CO yield, NO_x yield and temperature; the CO₂ yield was almost the same at different temperatures. The NO_x yield and fuel-N conversion ratio decreased with temperature increasing. The NO_x concentration maximum was the greatest at 800 °C. In the present experimental conditions, the optimum combustion temperature was 900 °C for RDF.

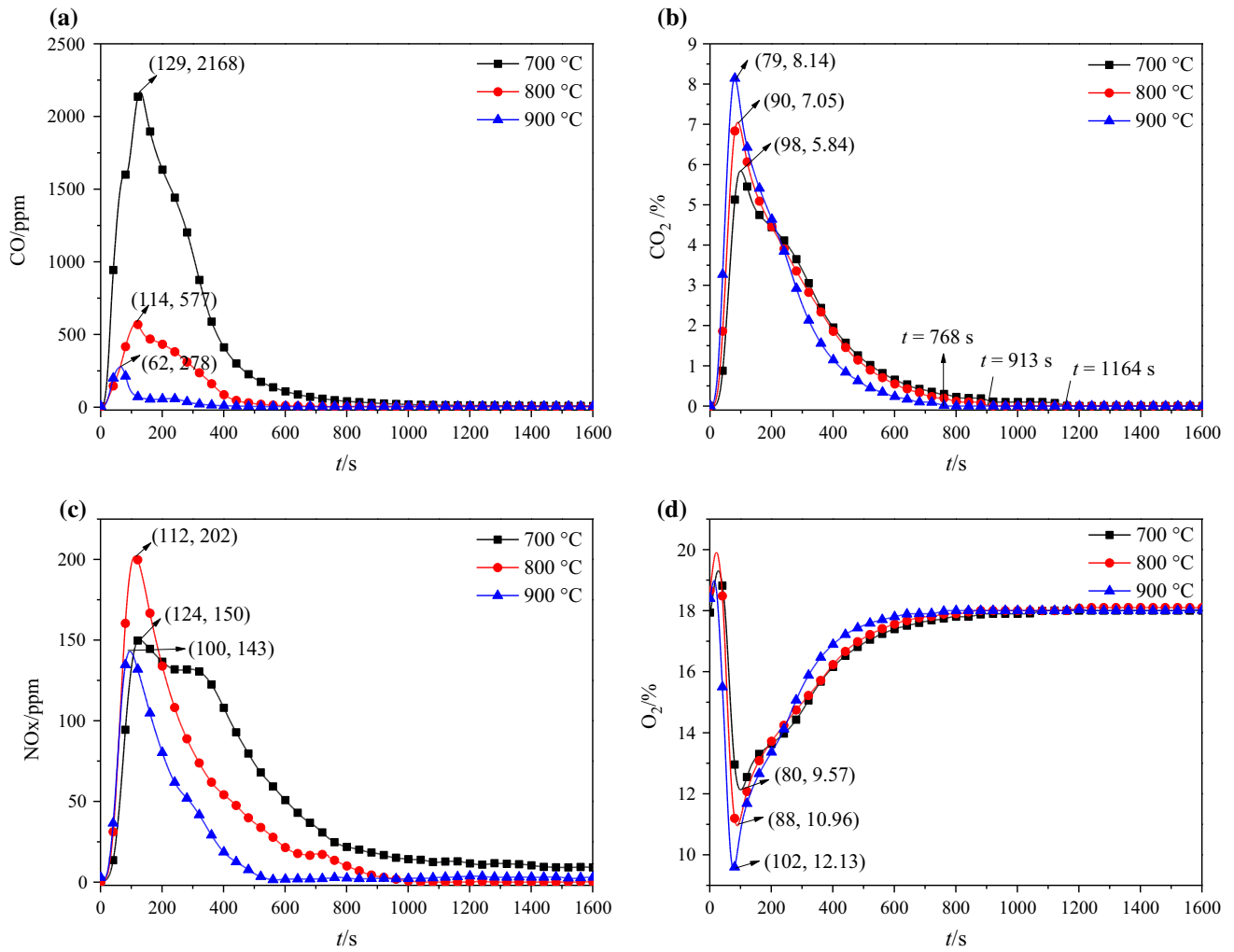


Fig. 5 Gas emission curves at different temperatures during RDF combustion. a CO, b CO₂, c NO_x, d O₂

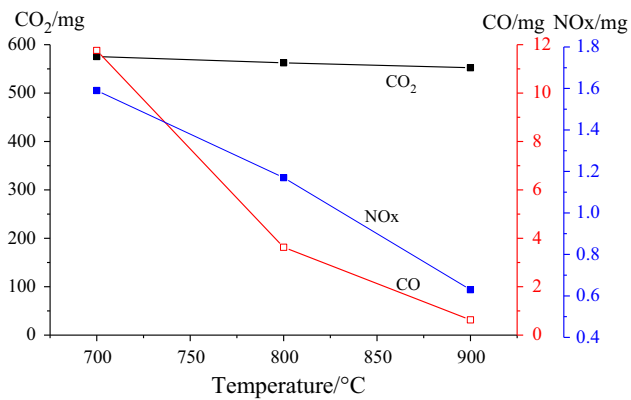


Fig. 6 Gas yields at different temperatures during RDF combustion

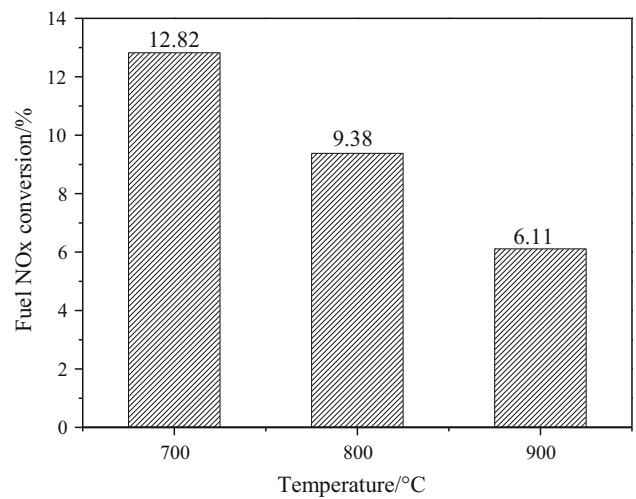


Fig. 7 Fuel-N conversion to NO_x during different RDF combustion at different temperatures

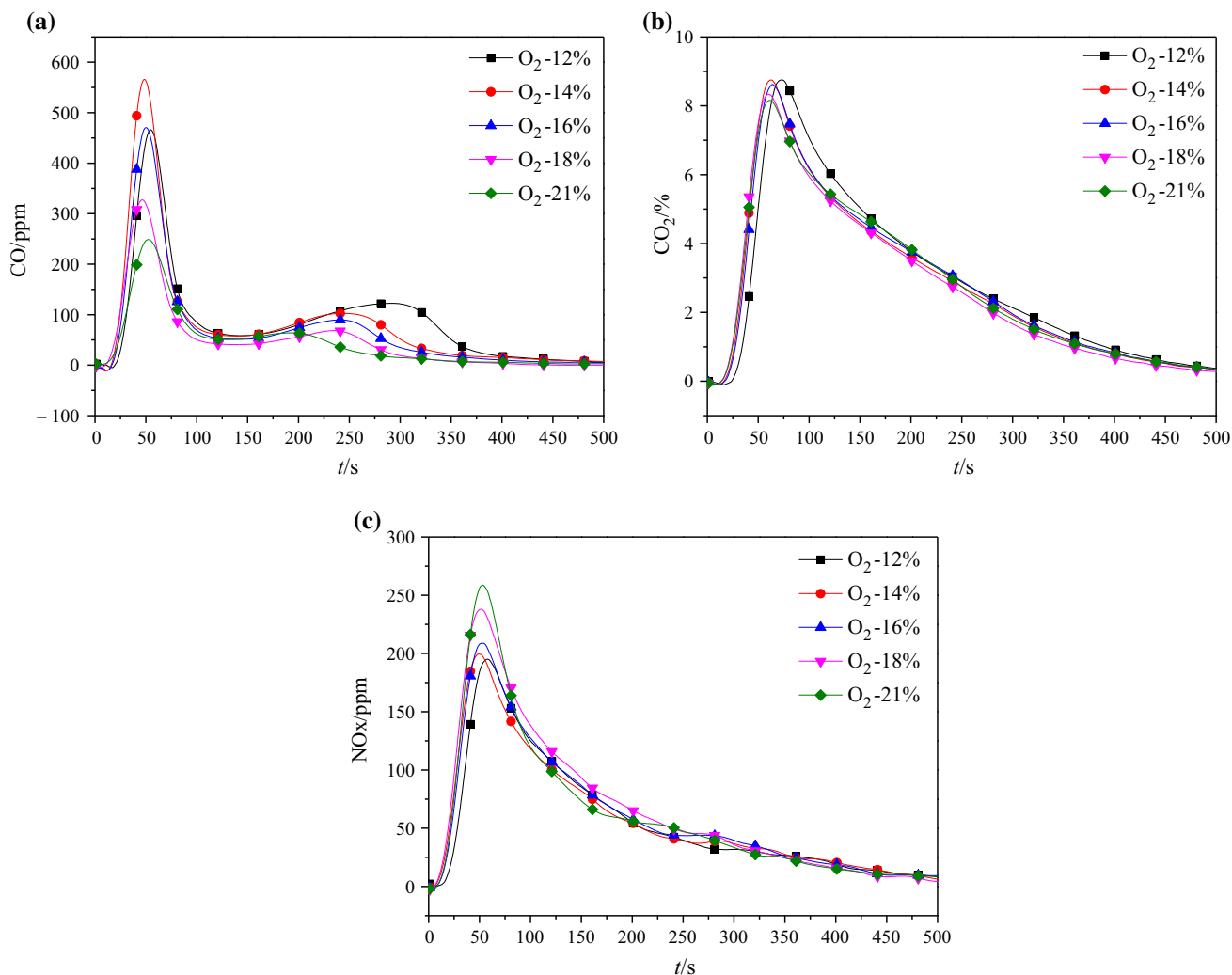


Fig. 8 Gas emission curves at different oxygen concentrations during RDF combustion. a CO, b CO₂, c NOx

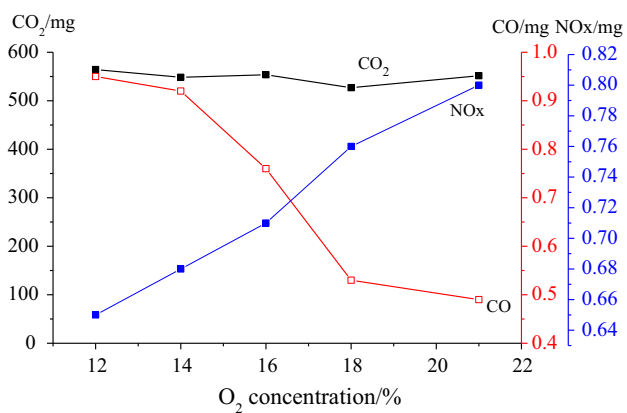


Fig. 9 Gas yields at different oxygen concentrations during RDF combustion

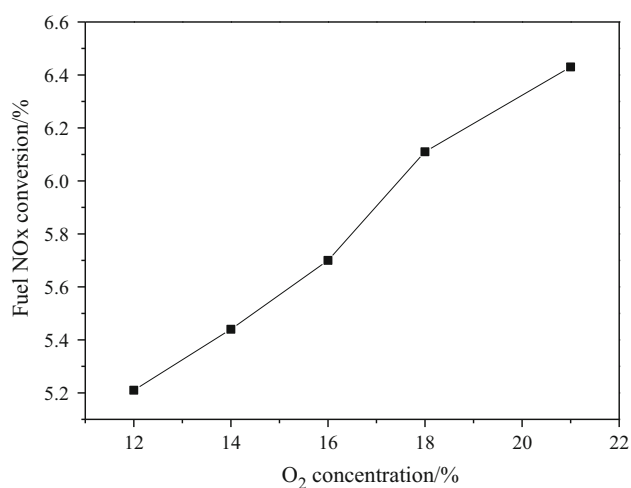


Fig. 10 Fuel-N conversion to NOx during RDF combustion at different oxygen concentrations

Effects of oxygen concentration on NO_x emission

Figure 8 shows the gas emission curves at different oxygen concentrations (12%, 14%, 16%, 18%, 21%) during RDF combustion at 900 °C. Figure 9 is the gas yields at different oxygen concentrations during RDF combustion. Figure 10 is the fuel-N conversion to NO_x during RDF combustion at different oxygen concentrations.

According to Fig. 8a and b, when the oxygen concentrations were 21% and 18%, RDF burned rapidly and the CO and CO₂ release peaks formed quickly. When the oxygen concentrations were 16% and 14%, RDF burned slowly and the volatile-CO and char-CO maximum concentration were higher than when the oxygen concentrations were 21% and 18%. When the oxygen concentration was 12%, the volatile-CO maximum and volatile-CO₂ maximum formed later. And the volatile-CO maximum was much lower when the oxygen concentration was 12% than when the oxygen concentrations was 14%. In general, the volatile-CO yield at O₂ 14% was much higher than other conditions.

Combining with Figs. 9 and 10, the CO yield decreased with oxygen concentration increasing. The CO₂ yield was about 580 mg at different oxygen concentrations. The NO_x emission maximum increased from 195 to 258 ppm with oxygen concentration increasing. And when O₂ concentration was 12%, 14%, 16%, the NO_x emission maximum was similar. In conclusion, the CO formed during combustion could inhibit the fuel-N being oxidized into NO_x. The NO_x yield and fuel-N conversion were very high when the oxygen concentrations were 21% and 18%. So the RDF should not be injected into the precalciner at the zone where oxygen concentration was 21% and 18%. On the other hand, when the oxygen concentration was low, for example, 12%, although the NO_x yield and fuel-N conversion was low, the combustion rate was quite slow which may result in the incomplete combustion of RDF in the precalciner. In general, when the oxygen concentration was 14%, the NO_x yield and fuel-N conversion was low and the combustion rate was close to when the oxygen concentration was 21% and 18%. There was a large amount of CO emission when the oxygen concentration was 14%, which could inhibit the NO_x formation during RDF combustion and could reduce the NO_x came from the rotary kiln. Therefore, the optimum oxygen concentration was 14% for RDF combustion.

Conclusions

Based on the TG-FTIR and Py-GC/MS, the RDF pyrolysis process included three parts. The first stage (< 200 °C) was the drying process and the decomposition of some biomass

components. The second stage (200–550 °C) was the release of most of volatiles. In the last stage (> 550 °C), some stable macromolecular matters released and some carbonate decomposed. A large amount of carboxylic acids and alkenes formed with NO_x at 200–550 °C. Thus, the hydrocarbon could inhibit NO_x production and promote the de-NO_x, and RDF could be used as an alternative fuel for de-NO_x in the cement industry.

By simulating the environment of the precalciner using a self-developed horizontal fixed-bed reactor, the combustion process and NO_x formation characteristics of RDF pyrolysis and combustion were studied. The effects of temperature (700 °C, 800 °C and 900 °C) and oxygen concentration (12, 14, 16, 18 and 21%) were studied.

(1) The fuel NO_x formation process was consistent with coal combustion process, involved two stages, including volatile NO_x and char NO_x. The volatile-N was the more dominant reactant source of NO_x emission. During the combustion process, the CO formed more easily than CO₂ and volatile NO_x. And the NO_x concentration reached the maximum during the decreasing of CO.

(2) Fuel-N conversion and NO_x emission yield decreased with temperature increasing from 700 to 900 °C, and the fuel-N conversions were 12.82%, 9.38%, 6.11%, respectively. At 900 °C, the combustion rate was rapid, and fuel-N in RDF could not be oxidized into NO_x in time, the NO_x yield and fuel-N conversion was quite low.

(3) Fuel-N conversion increased from 5.21 to 6.43% with oxygen concentration increasing from 12 to 21%. When the oxygen concentration was 12%, the combustion rate was too low. To ensure the low NO_x emission and high combustion efficiency, the optimum oxygen concentration for RDF combustion was 14%.

(4) In order to control the NO_x emissions in the precalciner during RDF combustion, the RDF should be injected at the zone with high temperature and low oxygen concentration. In the present experimental condition, the optimum temperature was 900 °C and oxygen concentration was 14%.

Acknowledgements This work was financially supported by the National Natural Science Foundation of China under Grant 51502221.

References

1. Mustafa K, Esin G, Yasemin T, Ufuk D, Senol Y, Volkan E. Development of refuse derived fuel for cement factories in Turkey. *Combust Sci Technol.* 2010;183:203–19.
2. Chen T, Zhan MX, Lin XQ, Li YQ, Zhang J, Li XD, Yan JH, Buekens A. Emission and distribution of PCDD/Fs and CBzs from two co-processing RDF cement plants in China. *Environ Sci Pollut Res.* 2016;23:11845–54.

3. Rahman A, Rasul MG, Khan MMK, Sharma S. Impact of alternative fuels on the cement manufacturing plant performance: an overview. *Procedia Eng.* 2013;56:393–400.
4. García AN, Marcilla A, Font R. Thermogravimetric kinetic study of the pyrolysis of municipal solid waste. *Thermochim Acta.* 1995;254:277–304.
5. Lin KS, Wang HP, Liu SH, Chang NB, Huang YJ, Wang HC. Pyrolysis kinetics of refuse-derived fuel. *Fuel Process Technol.* 1999;60:103–10.
6. Yi Q, Qi F, Cheng G, Zhang YG, Xiao B, Hu ZQ, Liu SM, Cai HY, Xu S. Thermogravimetric analysis of co-combustion of biomass and biochar. *J Therm Anal Calorim.* 2013;112:1475–9.
7. Mizuta R, Izato YI, Miyake A. Thermal ignition behavior of waste woods mixed with unsaturated fatty acids. *J Therm Anal Calorim.* 2015;121:1–9.
8. Coriolano ACF, Oliveira AAA, Bandeira RAF, Fernandes VJ, Araujo AS. Kinetic study of thermal and catalytic pyrolysis of Brazilian heavy crude oil over mesoporous Al-MCM-41 materials. *J Therm Anal Calorim.* 2015;119:2151–7.
9. Castro KKV, Figueiredo AL, Gondim AD, Coriolano ACF, Alves APM, Fernandes VJ, Araujo AS. Pyrolysis of atmospheric residue of petroleum (ATR) using AlSBA-15 mesoporous material by TG-FTIR and Py-GC/MS. *J Therm Anal Calorim.* 2014;117:953–9.
10. Stanislav H, Dagmar J, Adam C, Tomasz W. Gaseous components from pyrolysis-characteristics, production and potential for energy utilization. *J Therm Anal Calorim.* 2014;106:1–8.
11. Zhou H, Jensen AD, Glarborg P, Kavaliauskas A. Formation and reduction of nitric oxide in fixed-bed combustion of straw. *Fuel.* 2006;85:705–16.
12. Qian FP, Chyang CS, Huang KS, Jim T. Combustion and NO emission of high nitrogen content biomass in a pilot-scale vortexing fluidized bed combustor. *Bioresour Technol.* 2011;102:1892–8.
13. Duan F, Liu J, Chyang CS, Hu CH, Tso J. Combustion behavior and pollutant emission characteristics of RDF (refuse derived fuel) and sawdust in a vortexing fluidized bed combustor. *Energy.* 2013;57:421–6.
14. Francisco D, Changkook R, Vida N, Jim S. Combustion of refuse-derived fuel in a fluidised bed. *Chem Eng Sci.* 2007;62:627–35.
15. Akinori Y, Yuri K, Kenji K, Nelfa D, Kuniyuki K. In-situ monitoring of toxic heavy metals from RDF combustion by two-dimensional atomic absorption spectrometry. *Combust Sci Technol.* 2010;183:1297–307.
16. Crujeira T, Lopes H, Abelha P, Sargaço C, Gonçalves R, Freire M, Cabrita I, Gulyurtlu I. Study of toxic metals during combustion of RDF in a fluidized bed pilot. *Environ Eng Sci.* 2005;22:241–50.
17. Ferrer E, Aho M, Silvennoinen J, Nurminen RV. Fluidized bed combustion of refuse-derived fuel in presence of protective coal ash. *Fuel Process Technol.* 2005;87:33–44.
18. Wagland ST, Kilgallon P, Coveney R, Garg A, Smith R, Longhurst PJ, Pollard SJT, Simms N. Comparison of coal/solid recovered fuel (SRF) with coal/refuse derived fuel (RDF) in a fluidised bed reactor. *Waste Manag.* 2011;31:1176–83.
19. Dong TT, Lee BK. Analysis of potential RDF resources from solid waste and their energy values in the largest industrial city of Korea. *Waste Manag.* 2009;29:1725–31.
20. Genon G, Brizio E. Perspectives and limits for cement kilns as a destination for RDF. *Waste Manag.* 2008;28:2375–85.
21. Miskolczi N, Buyong F, Williams PT. Thermogravimetric analysis and pyrolysis kinetic study of Malaysian refuse derived fuels. *J Energy Inst.* 2016;83:125–32.
22. Grammelis P, Basinas P, Malliopoulou A, Sakellariopoulos G. Pyrolysis kinetics and combustion characteristics of waste recovered fuels. *Fuel.* 2009;88:195–205.
23. Sorum L, Gronli MG, Hustad JE. Pyrolysis characteristics and kinetics of municipal solid wastes. *Fuel.* 2000;80:1217–27.
24. Hill SC, Douglas SL. Modeling of nitrogen oxides formation and destruction in combustion systems. *Energy Combust Sci.* 2000;26:417–58.
25. Velden MVD, Baeyens J, Dougan B, McMurdob A. Investigation of operational parameters for an industrial CFB combustor of coal, biomass and sludge. *Particuology.* 2007;5:247–54.
26. Bosch H, Jamssen F. Formation and control of nitrogen oxides. *Catal Today.* 1988;2:369–79.
27. Zhong BJ, Roslyakov PV. Study on prompt NO_x emission in boilers. *J Therm Sci.* 1996;5:143–7.
28. Song Y, Beer J, Sarofim A. Nitric oxide formation during pulverized coal combustion. *Combust Sci Technol.* 1982;28:31–40.